

GLOBAL EARTHQUAKE SATELLITE SYSTEM

GESS



A 20-YEAR

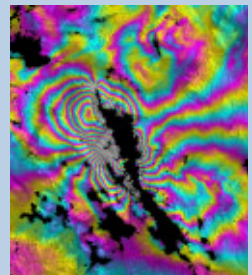
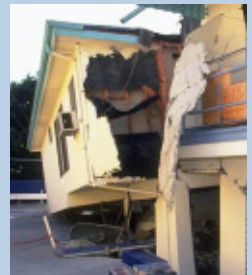
PLAN TO

ENABLE

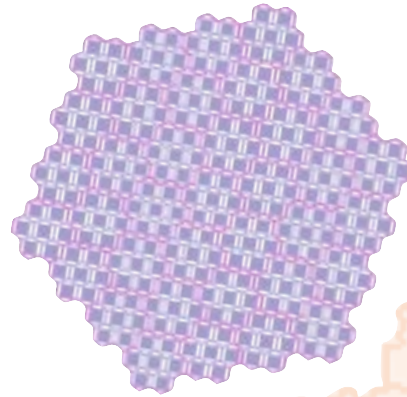
EARTHQUAKE

PREDICTION

MARCH 2003



Technology Studies



C H A P T E R S I X

CESS has studied SAR constellations from low-earth to geosynchronous orbits. These SAR missions place a significant demand on the spacecraft resources (mass, power, data rate). Revolutionary antenna technologies are required to enable the GEO and MEO systems described. High-efficiency integrated (single-chip) T/R modules are necessary to ensure the mass, power, and cost of the modules are not prohibitively high when thousands of modules are required. Adaptive scanning and phase self-compensation techniques will be necessary to alleviate requirements on antenna flatness. Modular or distributed architectures will enable these systems to be very flexible. Radiation-tolerant electronics are also a major challenge, particularly for the antenna electronics, which have only limited shielding.

For the GESS study, three technology studies were completed to address the need for large deployable electronically steered antennas and for a general reduction of radar instrument mass and power. By ultimately reducing the instrument cost, SAR constellations could be enabled. The three tasks were:

- Low-Power Chirp Generator: Demonstrate a miniaturized, low-power, rad-hard chirp generator, which is modular and flexible such that the design is directly applicable to GESS as well as other high-performance radar missions.
- High-Efficiency Transmitter Module: Demonstrate an ultrahigh-efficiency L-band Class-E/F amplifier for use in phased-array transmit/receive modules.
- Geosynchronous SAR Antenna: Conduct design and technology trades to establish the geosynchronous SAR antenna architecture to assess overall mission feasibility and identify the technology roadmap.

Low-Power Chirp Generator

The goal of this activity was to reduce the power consumption of the chirp generator by a factor of five from similar SIR-C/SRTM hardware. In this task, we have demonstrated a low-power, high-bandwidth, reconfigurable digital chirp generator (DCG) for use as a basic building block scalable to a variety of system applications.

Many NASA radar systems operate at L-band or include an L-band intermediate frequency as part of a higher-frequency system. Linear FM chirp waveforms are used for pulse compression. For signal repeatability and flexibility, DCG technology was chosen. The DCG must be frequency agile with the ability to switch between frequencies in a few nanoseconds. The DCG should produce spectrally pure signals (high spurious free dynamic range) and capable of 80-MHz chirp bandwidth.

Minimizing the DC power consumption was a major design goal. When distributed signal generation is required, such as in radar systems implementing an active array antenna requiring hundreds or even thousands of individual DCGs, then power considerations are paramount.

A final major design goal was to ensure that the DCG would endure the space environment. A combination of radiation testing and consultations with radiation testing experts was performed to address this issue.

Technical Challenges

Two candidate technologies were evaluated. The first was based on gallium arsenide (GaAs) technology (STEL-2375A) and the second was based on silicon CMOS technology (AD9854). The differing fabrication process of these two devices leads directly to

almost all of their respective strengths and weaknesses. High-frequency and high-bandwidth digital synthesizers must run at very high frequencies to satisfy the Nyquist limit. High-frequency digital systems invariably require more power than those of lower operating frequencies do. GaAs can run at speeds considerably higher than CMOS, but also consumes more power. Also, the power requirements for GaAs are practically independent of its operating speed. Therefore, one cannot choose to reduce power simply by reducing the speed. In contrast, CMOS requires less power to operate, and its power consumption is directly related to its operating speed, although it cannot run at the maximum speeds of GaAs. If a particular radar system requires less bandwidth, the AD9854 device may be run at slower speeds. In comparison, the STEL-2375A requires 15 W regardless of clocking speed or output frequency.

The AD9854 is hampered by its lower maximum frequency output of 120 MHz. While 120 MHz easily covers the required 80-MHz bandwidth, the signal must be “mixed up” to L-band through heterodyning. A fundamental problem with upconverting low-frequency signals is the close-in image frequency. Unless a multiple-stage upconversion approach is adopted, the image filter is often difficult to realize. The AD9854 is able to overcome this disadvantage by having In-phase and Quadrature (IQ) outputs. These signals can be fed into an IQ mixer to cancel the undesired side band. One technical challenge is created when using IQ modulation. The IQ outputs must be matched to a quadrature mixer that can handle DC-120-MHz input and L-band output. A survey of available components revealed this to be a non-trivial challenge.

A major challenge for the AD9854 is its radiation susceptibility. While the STEL-2375A is inherently rad-hard, the reliable operation of the AD9854 in a high-radiation environment is of concern. This is because it is a silicon (rather than GaAs) device using a commercial (non-rad-hard) fabrication process.

Enabling Technologies

Two semiconductor technologies were evaluated for use as the core-component of a low-power, rad-hard DCG. The first DCG-core is the ITT Microwave (formerly Stanford Telecom) STEL-2375A, which is a hybrid microcircuit composed of a GaAs numerically controlled oscillator (NCO) and

a CMOS DAC. The NCO performs all of the basic functions of the DCG and the DAC converts the digital signal to an analog waveform. The NCO runs up to 1 GHz, which means it can faithfully produce an analog signal up to 400 MHz. The second DCG-core is the Analog Devices AD9854, which is a 0.35- μm CMOS device. This device runs up to 300 MHz, which means it can faithfully produce an analog signal up to 120 MHz.

The STEL-2375A uses advanced high-speed digital GaAs technology. This technology is newer than silicon technologies, such as CMOS, but mature enough to have an established record. GaAs is well suited for space-based missions as it is naturally radiation tolerant, and its reliability has tested well. Newer materials, such as silicon germanium (SiGe), may become a more practical alternative as speeds increase. However, the radiation susceptibility of SiGe is currently unknown.

The AD9854 device is not new, but its new 0.35- μm CMOS fabrication process allows for high speeds and unique capabilities. Recent advances in well-balanced, high-frequency SiGe quadrature mixers have enabled us to take advantage of the quadrature outputs of the AD9854.

Results

The STEL-2375A and the AD9854 were each prototyped using an FPGA as an interface and controller. The DCG based on the STEL-2375A is shown in Figure 6.1(a) and the DCG based on the AD9854 is shown in Figure 6.1(b). Testing of these devices included DC power consumption over all operating modes, spurious free dynamic range, and features testing (i.e., chirp, CW, standby modes). Radiation testing was also performed on the AD9854.

Figure 6.1
Digital chirp
generators.



(a) STEL-2375A digital chirp generator.



(b) AD9854 digital chirp generator.

	SRTM DCG	STEL-2375A DCG	AD9854 DC
DC Power (typical)	25 W	15 W	3 W
Reference Clock (max)	180 MHz	1000 MHz	300 MHz
Bandwidth (max)	72 MHz	400 MHz	120 MHz
SFDR (measured worst case)	-36 dBc	-40 dBc	-52 dBc
Fabrication	GaAs	GaAs and CMOS XFCB process	0.35 μ m CMOS TSMC process

Table 6.1
Comparison
of devices.

As expected, the power requirement for the GaAs STEL-2375A was constant over all modes (CW or chirp), clocking speeds, and RF power out. Also as expected, the power requirement for the CMOS AD9854 was directly proportional to the clocking speed of the device. The AD9854 device also draws considerably less power when certain programmable modes are disabled such as the “inverse sinc” function. This flexibility can be used to optimize the device for low power, based on the specific performance needs of the system.

Performance results for both devices are listed in Table 6.1, and compared to the performance of the SRTM DCG, which is based on an earlier version of the STEL device.

Consultations with radiation testing experts at JPL indicate that the STEL-2375A, which is a GaAs device in a mil-spec package, is very likely to pass radiation tests without problems; therefore, radiation testing of this component was not performed. The AD9854, however, is a commercial CMOS device in a plastic package and there were concerns as to whether it can be space qualified. Therefore, limited radiation testing of the AD9854 was conducted.

Two tests were performed on the AD9854. The first was a total-dose-until-failure or Total Ionizing Dose (TID) test that was used to estimate of the component’s on-orbit life-time. The device was then subjected to heavy ions during operation. From this test, the rate and effect of single-event upsets (SEUs) on the device was estimated. Also, the device’s susceptibility to latch-up was estimated.

Results indicate this component is a candidate for flight integration at moderate to high risk, which is a lower risk level than that of components currently in some flight programs. The major risk factor for this device is damage to the device due to latch-up events; however, this may be mitigated through the addition of latch-up detection circuitry. The SEU rate is insignificant relative to the refresh rate of the device (>1000 times per second), and poses little risk. The part was tested to a TID of 200 krad without failure, but showed signs of degradation (high current draw) at 50 krad. The results of these tests are summarized in Table 6.2.

Summary and Conclusions

Two candidate technologies were evaluated for use in a general-purpose digital chirp generator. Desired features include low power

Table 6.2
Tests performed
on AD9854 DCG.

TEST	METHOD	RESULT
On-orbit lifetime	Total Ionizing Dose (TID)	50 krad
Single-event upset (SEU)	Heavy ions	6 per day (max)
Latch-up	Heavy ions	1 per 5 years (est.)

consumption, high speed, high dynamic range and high radiation tolerance. Flexibility of the waveform characteristics and performance is also very desirable, so that the device can be programmed for optimal performance with minimal power consumption. The AD9854 NCO-based digital chirp generator has all of these features. It significantly reduces power consumption. The SFDR performance is also superior to that of the STEL-2375A. Although the AD9854 is hampered by its lower speed, if the quadrature upconversion scheme can be shown to be reliable, then the AD9854's speed disadvantage can be overcome. The last obstacle for using the AD9854 in flight is its ability to operate reliably in a radiation environment. The limited radiation testing performed has determined that the AD9854 may be a viable option for some space applications.

If necessary, the AD9854 chip can be obtained in die-form and then repackaged for better radiation tolerance. For advanced systems, a custom application-specific integrated circuit (ASIC) device with similar performance could be developed using more advanced materials, such as silicon germanium (SiGe). This would also lead to significant reductions in the size of the device and could enable its use in a distributed antenna architecture, where the signal generators are distributed within the array.

High-Efficiency Transmitter Module

Future SAR missions, such as the concepts currently being studied at LEO, LEO+, and geosynchronous orbits, require very powerful radar systems. This task addressed the need for higher-efficiency transmitters for use in these advanced radar applications. Significant improvements in the transmit/receive (T/R) module efficiency will make very large, high-power, electronically scanned SAR antennas more feasible and affordable.

Existing and recently proposed L-band SAR systems (RADARSAT-2, SIR-C, SRTM, LightSAR, ECHO) all rely on conventional Class-AB or Class-C power amplifier technologies to achieve moderate L-band efficiencies of 30–40%. By using the new Class-E/F power amplifier circuit topology, efficiencies on the order of 70–90% can be achieved. Using current solid-state power amplifier (SSPA) technology, 60 kW of radiated RF power (at 20% duty cycle) will require roughly 30 kW of DC power for the transmitter alone. By improving this efficiency to 80%, the DC power requirement is reduced to 15 kW, thus requiring a much less capable spacecraft and dramatically reducing the mission costs. By miniaturizing the high-efficiency T/R modules, they can be used for both conventional rigid panel phased-array antennas (LEO, LEO+ SAR missions) as well as in super-lightweight, flexible membrane antennas (geosynchronous SAR).

Significant improvements in efficiency will also simplify the thermal design and increase reliability, particularly for membrane antennas, where heat dissipation is far more challenging.

The objective of this study was to demonstrate the feasibility of using a Class-E/F power amplifier at L-band frequencies. The design goals were to achieve 30 watts at L-band (1.25 GHz) with greater than 80 MHz bandwidth and 70% efficiency.

Technical Challenges

We have studied the use of switch-mode amplifier circuits for use as high-efficiency RF power amplifiers. Switching amplifiers, such as Class-E and Class-E/F amplifiers, use the active devices as switches. That is, the active device is ideally fully-on (short-circuit) or fully-off (open-circuit). These circuits are commonly found in switching power supplies, but only recently have they been exploited as RF amplifiers due to the availability of transistors with substantial gain and power at microwave frequencies. The theoretical efficiency for Class-E and Class-E/F amplifiers is 100%; practical efficiencies of 70–90% have been demonstrated at UHF frequencies.

To achieve ultrahigh efficiency, there are four primary loss mechanisms to overcome: conduction loss, input power loss, discharge loss, and passive component loss. The first three loss mechanisms are due to the active devices. Active device losses for switch-mode amplifiers occur mainly during transitions from one switch state to another. By using a high-Q resonant output network, Class-E and Class-E/F amplifiers minimize this switching loss. At L-band, the active devices are typically large in size, have large on-resistance, large output capacitance, and very low

input impedance — all contributing to the loss. The last loss mechanism is due to the passive matching networks. Due to the topology of the push-pull amplifier, a microstrip balun (balanced-to-unbalanced transformer) circuit was needed to convert from a single-ended to double-ended signal at the input and output. This balun must be very low loss and also must be small and planar with a flexible geometry for easy integration into the amplifier circuit. Proper modeling of parasitic capacitance and inductance was another important challenge to ensure the circuit can be properly designed and reproduced to the given requirements.

Enabling Technologies

The California Institute of Technology (Kee et al., 2001) has developed a new class of power amplifier, the Push-Pull Class-E/F power amplifier. The Class-E/F amplifier, which is similar in operation to the more common Class-E amplifier, promises to further increase efficiency and reduce circuit complexity while extending the maximum operating frequency and bandwidth to L-band and beyond.

Push-Pull Class-E/F amplifiers have the following advantages over other switching amplifiers:

- They combine two transistors so higher power levels can be achieved.
- They incorporate the transistor output capacitance into the tuning circuit. Since most high-power devices have high-output capacitance, this feature improves the performance of the tuning circuit.
- They have a lower peak voltage, reducing the transistor breakdown voltage requirement.
- They have lower RMS current, which reduces resistive loss of the circuit.

- They have soft-switching, which keeps the current at a low level while the capacitors discharge, reducing the discharging loss of the amplifier.

The extension of the Class-E/F circuit topology to higher frequencies and high output powers (over 20 W) requires careful selection of the power transistor device. LD-MOS, SiC, and GaN are all viable technologies. For this demonstration, LDMOS (specifically, the Motorola MRF284) has been selected because of its low cost and availability. The advantages of LDMOS include high breakdown voltage and high operation frequency. GaAs is also a mature and widely available device technology. Wide-bandgap materials, such as SiC and GaN, also show promise for high-frequency and high-power applications. However, since these technologies are not as mature as LDMOS and GaAs, the availability of commercial products is a practical problem.

Results

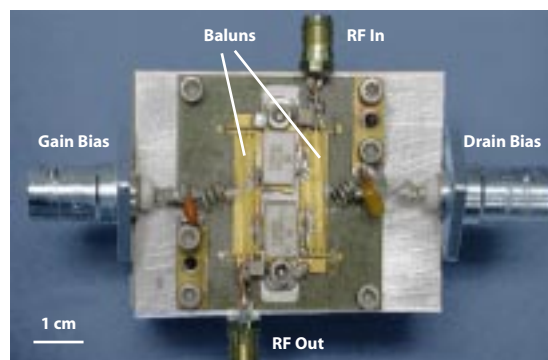
An L-band Class-E/F power amplifier (PA) has been built and measured (Figure 6.2). Preliminary results show an efficiency of 64%

at 800 MHz and an output power of 30 W. The operating frequency is less than the target 1250 MHz, which may be due to parasitic capacitance and inductance in the circuit. Future work includes more thorough testing of the amplifier. In addition, improvements to the circuit models are required to adjust the operating frequency. Since the active devices are the most critical components of the amplifier, evaluation of different device technologies (LD-MOS, GaAs, SiC, GaN) should also be addressed in future studies.

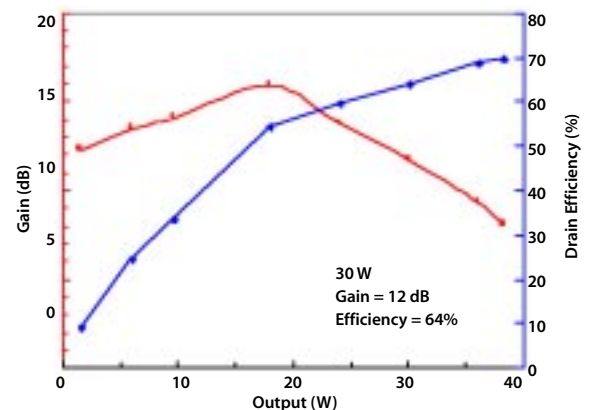
Summary and Conclusions

In this task, JPL teamed with Caltech to explore the use of the new Class-E/F amplifier as an L-band transmit module to achieve high efficiency. Although the performance goals were not entirely achieved, this proof-of-concept breadboard has demonstrated the feasibility of using Class-E/F amplifiers at L-band. This research will continue through an Earth Science Technology Office (ESTO)-sponsored technology research task under the Advanced Component Technology (ACT) program. Future research will include improv-

Figure 6.2
(a) Photo of the L-band Class-E/F PA.
(b) Output power, efficiency, and gain of PA at 800 MHz.



(a)



(b)

ing the circuit models to better predict the performance and then demonstrating improved performance at L-band. Ultimately, through the ACT program, the Class-E/F PA will be incorporated into a complete high-efficiency L-band T/R module.

Geosynchronous SAR Antenna Study

Future advanced SAR concepts, such as the one being studied by GESS for a geosynchronous SAR mission, require very large antenna apertures with full 2-D beam-steering capability. This class of antennas requires apertures on the order of several hundreds of square meters transmitting 60 kW of RF power. For this class of mission to be feasible and affordable, the antenna mass and stowed volume must be low enough to fit into an existing launch vehicle. Antenna mass densities must be reduced by an order of magnitude (20 kg/m² to less than 2 kg/m²).

Several notional concepts were developed for a geosynchronous SAR mission and two were studied in some detail. The first concept is to deploy this system using autonomous, reconfigurable panels. Here we envision using an array of hexagonal panels that can be assembled in space to form arrays of differing geometries. Therefore, the same basic antenna element can be manufactured in large volumes on the ground and then assembled in space in the desired configuration. These autonomous antenna panels would be completely self-contained each with its own spacecraft avionics and solar arrays. A detailed study of this concept was conducted for the National Reconnaissance Office (NRO) under the Director's Innovation Initiative (DII) program. The second concept under consideration for the geosynchronous SAR system is a large deployable hexagonal antenna with centralized (rather

than distributed) spacecraft bus components, as described in Chapter 4. The advantage of this concept is that a single launch vehicle can deploy the entire array. The autonomous panel concept would require multiple launches to deploy an antenna of the size required for GESS.

A design study was completed of the geosynchronous SAR antenna based on the large deployable antenna concept to identify key technology drivers for such a system. First, several antenna architectures were evaluated. Once the antenna architecture was selected, a study of the signal generation, distribution, and transmit/receive architecture was conducted to optimize for low mass, low power, and maximum performance. Antenna structures and deployment were also studied. Based on these design and technology trades, the antenna mass, power, and cost were estimated. The design was then used in a Team X exercise to assess overall mission feasibility. This section summarizes the results of the antenna design study.

Antenna Requirements and Performance

The geosynchronous SAR mission design concept was presented in Chapter 4. The driving requirements of the radar antenna are presented in Table 6.3. For a large 30-m aperture antenna and 2-D beam scanning capability, mass, cost, and complexity are major factors to be considered in selecting the antenna architecture. Because the required amount of beam scan is 8° and possibly greater for other future systems, only array concepts are considered for wide-angle beam scanning needs.

Three array concepts were considered for performance trade-off: distributed phased array, reflectarray, and array lens. The distrib-

Table 6.3
Geosynchronous
SAR antenna
requirements.

PARAMETER	REQUIREMENT
Frequency	1.25 GHz
Bandwidth	80 MHz (6.5%)
Aperture Size	30 m × 30 m
RF transmit power	60 kW
Duty cycle (PW*PRF)	20%
Beam scan	±8° or more
Polarization	Single linear vertical
Sidelobe level	-30 dB
Cross-pol level	-25 dB

uted phased array approach has graceful degradation in performance with very little risk of a single-point failure. Also, by using mostly corporate-feed power division, the array is able to achieve adequate RF bandwidth where more than 10% bandwidth can be achieved. The reflectarray and lens arrays do not require complicated beamformers (power dividers) but have limited bandwidth and require a high power TWTA. Using distributed T/R modules would be the more feasible and reliable approach to achieving the very high transmit power. The simplicity of the reflect-array and array lens approaches cannot overcome the bandwidth advantage of the distributed phased array. Because the 6.5% bandwidth is an essential requirement of the radar system, the more complex distributed phased-array approach is selected.

One of the most constrained aspects of the array architecture is the element location. The element locations will determine the overall sidelobe and grating lobes of the antenna. From the standpoint of complexity, it is

desirable to minimize the number of elements. However, insufficient element density causes the appearance of grating lobes and reduced gain when the beam is scanned. In order to minimize the element density while maintaining the required suppression of grating lobes, a triangular grid is used. By arranging the elements on the nodes of a triangular grid, slightly greater (as compared to rectangular grid) element spacing can be used. The maximum spacing that will meet the grating lobe requirements is 0.9λ , which is 21.4 cm at the center frequency. Suppression of grating lobes also requires that each element has its own phase shifter. A 4-bit phase shifter quantization should suffice to achieve the required beam pointing resolution and sidelobe level. To reduce the impact of phase shifter losses on system performance, each element is also fed by its own T/R module, which contains a low-noise amplifier (LNA), a PA, and control circuitry to ensure signal gain on the antenna element side of the phase shifter. An alternative architecture includes a T/R module (PA and LNA) at each subarray and only a phase shifter at every element. This architecture requires low-loss phase shifters. The “fully-populated” architecture delivers better performance but at a higher mass and cost. For this study, we have selected the fully-populated architecture with one T/R module per element.

In order for the 30-m antenna aperture to be stowed and fit into a several-meter launch vehicle fairing, the antenna’s membrane aperture must be separated into several sections of rollable and foldable structures. Because of the separation of structures and folding of membranes, gaps where there are no radiating elements (up to 10 cm wide) will be formed between membranes. In addition, because of the particular deployment mechanism

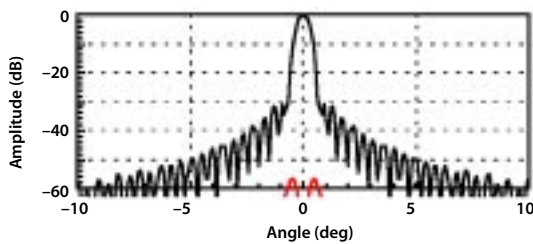
selected, the aperture center will have a 1-m-diameter circular hole where there also are no radiating elements. Far-field radiation patterns and antenna gain losses were calculated to predict the significance of gaps and holes. Figure 6.3(a) gives the 0° scanned pattern from a perfect 30-m aperture without any gap or hole. Figure 6.3(b) shows the pattern effect when gaps and center hole are present. It can be noticed that, besides a 2 dB rise in sidelobe level, there is no significant change in pattern shape. The antenna gain loss is 0.63 dB.

When the main beam is scanned to 8° from the broadside direction, the pattern effects are given in Figure 6.4(a) and (b). Again, no significant change occurred in the pattern. The gain loss is 0.72 dB. One can conclude that the presence of the given membrane gaps and center hole do not produce any detrimental radiation effect.

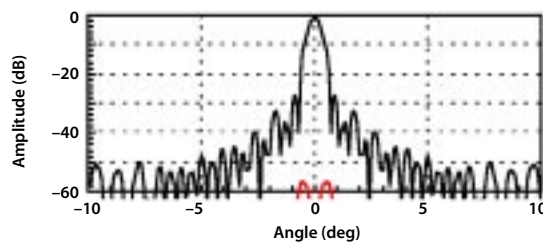
System Architecture

There are many architectural trade-offs, some of which depend upon the future development of technologies. The system architecture presented here incorporates current knowledge and technology predictions in order to satisfy the instrument requirements. However, in cases where the most effective choices are not clear, options are presented along with pros and cons of each approach.

Two key goals of this design are to minimize the overall system mass and to facilitate easy stowage of the antenna. Both of these goals indicate that we should minimize the number of antenna layers. The microstrip patch radiators require two layers (one for the patches and one for the ground plane); thus, the minimum number of layers is two. However, in order to have enough space to implement the required microstrip power dividers,

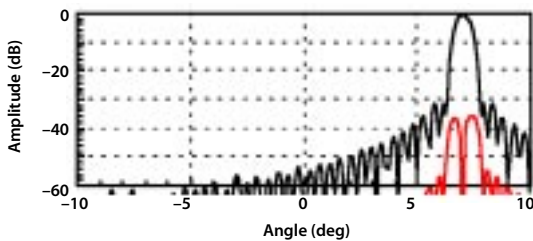


(a) Perfect aperture.

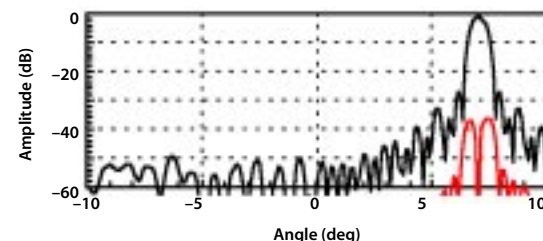


(b) With given gaps and center hole.

Figure 6.3
Calculated radiation patterns of a 30-m aperture array with 0° beam scan.



(a) Perfect aperture.



(b) With given gaps and center hole.

Figure 6.4
Calculated radiation patterns of a 30-m aperture L-band array with 8° beam scan.

a third layer is required. Each layer is constructed of 40- μm -thick polyimide dielectric material, such as Kapton[®], with copper metallization. In order to satisfy the skin depth requirements at L-band, the copper must be at least 5 μm thick. However, other requirements such as DC power distribution, heat dissipation, and radiation shielding may require that the metallization be thicker in some places.

There are two reasonable places to put the T/R modules: on the inner ground-plane layer or on the outer layer with the patch radiators. In order to minimize the number of interconnections, it is advantageous to place the T/R modules on the layer with the patches. From a thermal management perspective, it is best to place the T/R modules on the ground plane layer. This allows heat to be spread over the entire ground plane, increasing radiating area. However, each T/R module must then be connected to the patch, which would require over 15,000 interconnections, decreasing reliability and making assembly difficult and costly. A promising approach is to place the T/R module on the inner layer, as above but using a noncontacting method, such as coupled lines or apertures, to feed the T/R modules and the patches. This is superior from a mechanical and reliability perspective but may incur substantial RF losses, thereby degrading power efficiency and system performance. Because of the substantial advantages of this approach, it merits further investigation.

Because of the large size and operating bandwidth of the antenna, true time delays (TTD) are required for proper beam formation. If phase delays alone are used, a reduction in gain and increased grating lobes would

occur. It is impractical to apply a time delay to every element, so instead, the full array is broken up into subarrays of reasonable size and each subarray has a time delay applied to it. Additionally, each element within the subarray contains a controllable phase delay. The full array and subarray design is illustrated in Figure 6.5.

There are a total of 61 TTD subarrays. The size of the time-delayed subarray was chosen to minimize the degradation of antenna gain caused from grating lobes. Separation of the antenna into subarrays also facilitates signal distribution. Each of these TTD subarrays is composed of 36 groups of seven elements (defined as subarrays) arranged in a hexagonal pattern. All 252 elements in the subarray are driven by a single digital transceiver. The digital transceiver receives digital waveform data from a central controller and converts it to an analog waveform with the appropriate time delay and is distributed to the 252 elements with T/R modules and phase shifters. Received power from each element is combined in the microstrip divider/combiner networks so that a single L-band analog received signal reaches the digital transceiver. This signal is then digitized and the resulting data is sent back to a central processor/controller (CPC) for final beamforming. The array system architecture is shown in Figure 6.6, which illustrates the interconnection of the CPC, the TTD subarrays, the T/R modules, and radiating elements.

As previously noted, true time delay is required for proper beam formation. This can be achieved in either analog or digital circuitry. Analog time-delay circuitry consists of switched time delays that are implemented in transmission lines or optical fibers. Because of the line lengths involved, these delays are

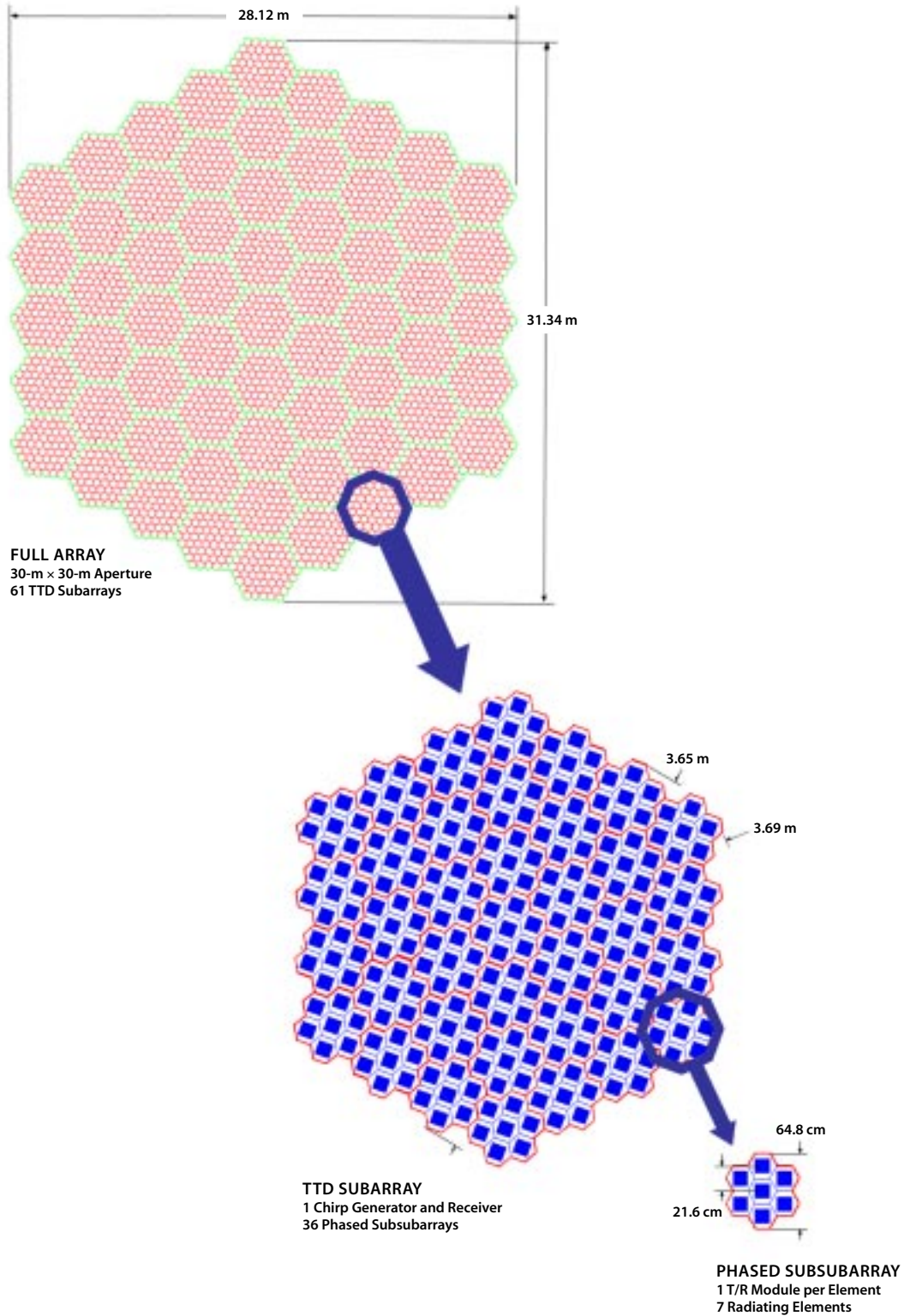
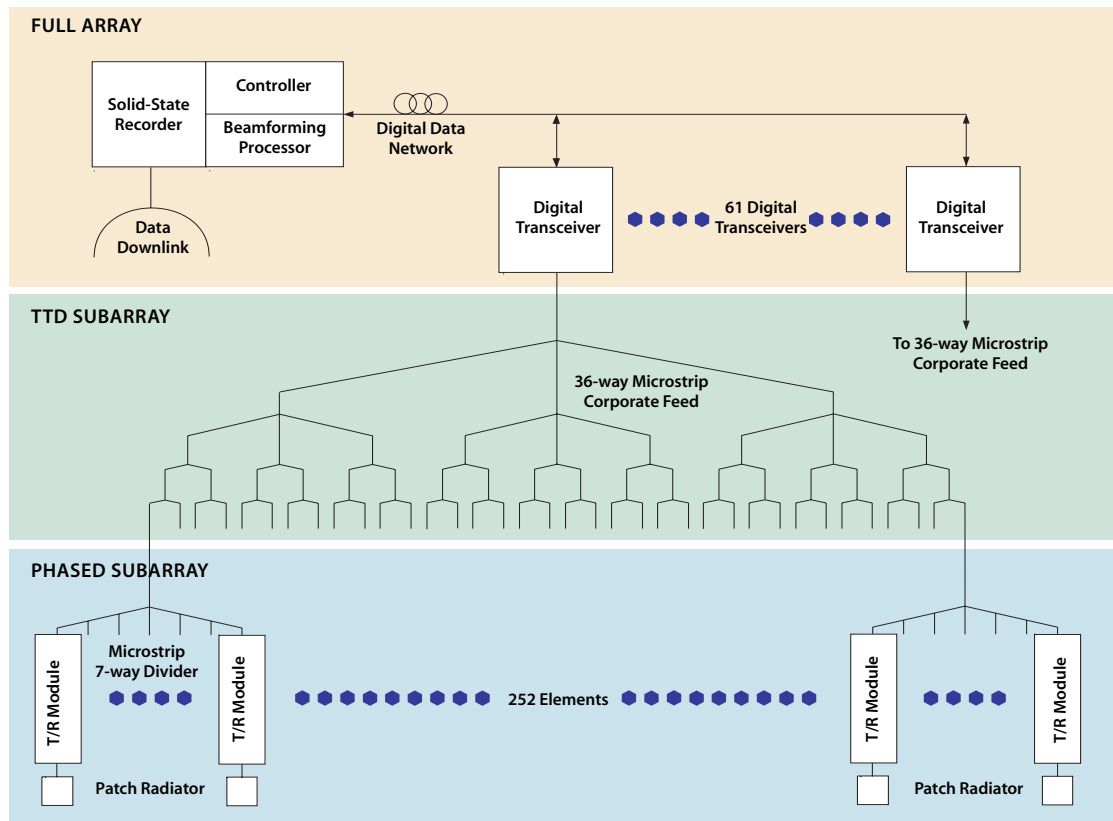


Figure 6.5
Array and subarray
configuration.

Figure 6.6
Array system
architecture.



difficult to miniaturize. Therefore, the approach chosen for this design is to implement the time delays digitally. The major challenge is developing a low cost method of integrating optical fibers with the membrane and reliable connection of fibers to the electronics. Also, because of the high radiation environment, radiation-tolerant fibers must be used.

The architecture of the T/R module is conventional in the sense that it contains a power amplifier, low-noise amplifier, phase shifter, programmable attenuator, and control circuitry. Because of the high average transmit power of the array, it is essential that the power amplifiers be as efficient as possible. Class-E and Class-F amplifiers with over 90% efficiency at 50 MHz have been demonstrated and efficiencies of 70% at L-band are

predicted. This is an area of ongoing research of great interest for both radar and communications applications. A separate activity was undertaken in the GESS study to demonstrate an L-band high-efficiency Class-E/F power amplifier for use in the T/R module, although it wasn't assumed in this system design.

While the architecture of the T/R module is conventional, its packaging is not. In order to successfully mount T/R modules on a thin membrane and maintain the ability to fold and roll it, the modules must have a low mass and a small footprint. Also, reliable and low-cost attachment techniques are required. This requires highly integrated mixed-signal electronics. In order to reduce the mass of the modules, radiation shielding must be minimized. This requires the use of highly radiation-tolerant semiconductor technologies.

Another challenging aspect of such a large and powerful array radar is generating and distributing electrical power. Power is generated by a skirt of flexible solar cells that wrap around the cone and at the edge of the array. Power is then fed inward from the perimeter of the array. In order to minimize ohmic losses in the power distribution systems, 100 V was chosen for the distribution voltage. Voltages greater than 100 V run a substantially increased risk of arcing, while lower voltages will increase ohmic losses. Since the electronics in the T/R module and digital transceivers require lower voltages, voltage conversion is required.

Heavy copper wire attached to the membrane causes unwanted mechanical stresses and additional integration problems. Since achieving low-loss transmission requires a certain conductor cross-sectional area, we can minimize the thickness of conductors by maximizing the surface area that they cover. The ultimate extension of this approach is to feed the power through a thin copper sheet on the interior membrane layer. The sheet can be coated with copper on both sides, with one side being the power plane and the other side the ground plane. One danger of this approach is that a short circuit caused by damage to the membrane may disrupt the power source for the entire array. An approach to mitigate this risk is to divide the power plane into small cells, each connected to its neighbors by fusible links. This concept requires further study.

Structural/Mechanical

A structural system concept for deployment of the large antenna and integrated solar arrays was formulated. This included several trade studies on various deployable and inflat-

able booms and sizing of the structural members (vertical and horizontal booms). A study of system packaging, membrane management, deployment, and tensioning was conducted. A finite-element model was assembled and used in a preliminary structural analysis. The results of these studies were used to estimate the overall system mass and launch volume. The design was then used in a Team X exercise to assess overall mission feasibility. The results of the overall geosynchronous SAR mission design were presented in Chapter 4.

The horizontal booms deploy, support, and tension the membrane antenna aperture. The self-rigidizable spring-tape-reinforced (STR) inflatable booms of 10-inch diameter were selected for this application for high stiffness and low mass. Other high-stiffness, lightweight booms, including those deployed by mechanical means, are also suitable. The axially deployed booms must be very stiff to maintain aperture flatness. We have baselined the AEC-Able ADAM mast for this application since it has SRTM heritage. Able is currently developing an improved high-stiffness mast that will reduce the linear mass density to 1/8 of the SRTM mast and increase the stowed packaging efficiency by a factor of two while maintaining equivalent strength, stability, and stiffness. This advancement in technology will simplify the packaging of the geosynchronous SAR antenna and increase mass and launch volume margins.

Membrane Aperture Packaging

Membrane management was studied to identify a feasible method of packaging and deploying the antenna. The membrane antenna and the integrated ring-shaped solar array together form a dodecagon. Each of the

Figure 6.7
Antenna folding
procedure.



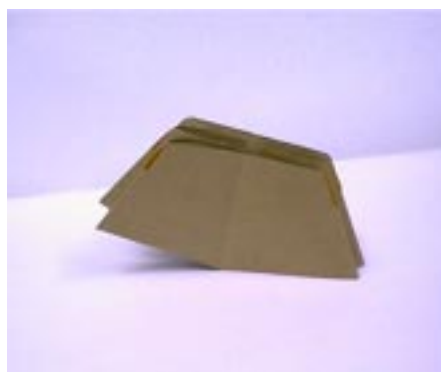
(a)



(b)



(c)



(d)

twelve sides of this dodecagon has a length of 19 meters. To package this dodecagon, it will be first divided by twelve radially extended fold lines and then be packed by a fold-and-roll method. The folding part of this packing method involves the sequential origami folding steps exemplified in Figures 6.7(a) through (d).

The folded stack height can be reduced by increasing the number of rings in the folding pattern while using the same folding approach. A four-ring folding will reduce the stack height to around 5.2 m. Although further reduction of stack height can be achieved by using even more rings, it may present other difficulties in packing the membrane aperture. Also, it is important that the RF design be made compatible with the fold lines as discussed previously. To stow for launch, the folded-up membrane stack will be rolled around the 1-m-diameter central mandrel that is also the canister housing the stowed upper ADAM mast.

Conclusions

While the implementation of a large-aperture, high-power, true time delay (TTD) radar array on flexible membrane presents many architectural challenges, none of the obstacles appear insurmountable. A key focus area for further research is interconnect technology. Lightweight, low-loss, membrane-compatible interconnects for RF, and data and power distribution must be developed. Furthermore, these interconnects must be highly reliable and easily manufactured. Continued research into membrane compatible electronics is also required. The ultimate goal is a low-cost, high-reliability process for producing highly integrated, radiation-hardened, mixed-signal circuits and attaching them reliably to a mem-

brane. This technology is critical for implementation of the GESS radar and would also enable many other large aperture radar concepts. Membrane antenna technology has been demonstrated with several successful ground demonstrations. Future research must address improved element feeding techniques such as slot-coupled to replace bulky feed-probes. This will result in a much less complex and easier to manufacture design that can stow much more compactly. The antenna structures can implement either mature mechanically deployable structures or the emerging technology of inflatable/rigidizable structures. The first few modes of the system are governed mainly by the stiffness of the horizontal booms. Preliminary analysis of the in-space dynamics of the deployed flight system indicates that the fundamental frequency is greater than 0.2 Hz using inflatable boom technology, which is well within the capability of typical spacecraft attitude control systems. The primary challenge is maintaining acceptable antenna flatness, and addressing calibration and metrology techniques to correct for surface deformation in the array.

Technology Roadmap

What are the challenges?

We have described a number of advanced SAR mission concepts. For the near-term missions (LEO and LEO+), there is little technology development required. Evolutionary advances in technology to reduce instrument mass and power will lead to incremental improvements in performance. However, to enable the most ambitious GESS mission concepts, such as the geosynchronous SAR constellation, revolutionary new technologies are essential. The antenna is the dominant component of the radar system and with the

increasing demands for higher resolution, higher sensitivity, targetability, and coverage, the antenna aperture becomes very large, requiring a complicated distributed active array architecture. The array architecture presents many system-level design and integration challenges. Since thousands of T/R modules are required, reducing the mass, power, and cost of these modules will be very beneficial. In addition, signal distribution (RF, control, power) is very complex and low-cost interconnect technologies are required to interface with the modules. Also for the large array, advanced techniques such as digital beamforming and TTD steering may be required. Adaptive methods to compensate for deformation in the array flatness will also need to be addressed. These system issues require a very complicated antenna. For such a large aperture to fit within existing launch vehicles, membrane antenna technology would likely be employed rather than conventional rigid panels. This is a major technical undertaking.

Inflatable membrane antennas have been an area of research over the past several years, with several engineering prototypes developed to demonstrate that inflatable structures can be used to deploy and stretch flat membrane antenna apertures with good RF performance (Huang et al., 1998). Recent focus on inflatable structures has been to develop self-rigidizing technologies and methods to control deployment. Approaches to properly tension the membranes to maintain flatness and precise layer separation is also an area of focus. Although inflatable membrane antennas have been successfully demonstrated, these antennas have not yet addressed the very complicated problem of integrating electronics within the aperture. Nor can the existing

systems be scaled to antennas of the size required for GESS. Mechanically deployed structures are far more mature than inflatables and have the advantage of high stiffness and stability; however, they do not have the high packing efficiency of inflatable structures. Trade-off studies indicate that as the structure length grows beyond 50 m, inflatable technologies may be advantageous. For GESS, both inflatable and deployable structures are candidates.

Besides the mechanical complications of constructing a large-aperture membrane SAR, the integration of the large number of T/R modules and other electronics within the membrane antenna (reliably and cost effectively) is also a major challenge. Since the ultimate goal is to keep the weight and stowed volume of the antenna small, conventionally packaged T/R electronics are not appropriate. Furthermore, attaching a large packaged component to a thin-film membrane also presents reliability concerns. Therefore, our vision includes embedding or attaching unpackaged chips directly to the membrane structure.

The current state-of-the-art T/R modules typically use three or four chips in a packaged hybrid microcircuit. A fundamental goal is to integrate all the T/R electronics onto a single chip. This will minimize the total part count and will result in overall reductions in module cost, assembly cost, and interconnect costs, while increasing reliability. This is particularly significant when tens of thousands of T/R modules are required.

Since the chip is not packaged (at least not in the same way a conventional T/R module is packaged), the radiation shielding of the chip becomes a serious issue. Because the chip is on a membrane, the heat dissipation from the T/R is also challenging. New membrane materials with better heat conductivity are

needed for passive cooling of the electronics. At high power levels, active cooling methods such as micromachined heat pipes or similar technologies may be required. These difficulties are mitigated when very high-efficiency T/R modules are used.

As advanced (lower TRL) technologies such as thin-film organic electronics mature, the possibility of printing some portions of the T/R electronics (i.e., passive components, phase shifters, sensors, etc.) directly onto the membrane may become possible. This would greatly simplify the complexity and construction of the antenna and may lead to a substantially lower production cost, which is key to a viable SAR constellation mission.

Current Technology Investment

NASA is actively working to develop the technologies required for large membrane antennas. Figure 6.8 and Table 6.4 show the roadmap for this effort. Currently two NASA programs, Code Y's ACT program and Code R's Advanced Measurements and Detection program, are sponsoring this effort. The GESS geosynchronous SAR antenna architecture study has been used to establish the technology requirements and roadmap for the long-term SAR missions. The near-term goal is to demonstrate a fully functional 2×8 element antenna subarray by 2004. The demonstration will combine some of the key technologies that we have been developing to ensure that the system as a whole is functional before more effort is spent on increasing the TRL of the technologies in use. Internal R&D funding is also supporting an independent task to develop a single-chip MMIC T/R module, which will ultimately replace the current five-chip modules.

COMPONENT	TECHNOLOGY	LEO+	MEO	GEO
Lightweight structures	High-stiffness deployment systems with high packing efficiency; inflatable/rigidizable and mechanically deployable structures; membrane tensioning.	CR	E	E
Large membrane antennas	Durable, low-loss, thin-film membrane antenna materials; array feed technique compatible with the membrane electronics and array architecture.	CR	E	E
Integrated, rad-hard, low-power electronics	Single-chip MMIC T/R module; low-power DCG; TTD devices; L-band digital receivers.	CR	E	E
High-power, high-efficiency transmitters	High-efficiency Class-E/F L-band T/R modules; Si, GaAs, SiC, and GaN power amplifiers.	CR	E	E
Low-loss, low-power phase shifters	MEMS or BST; space-qualification and reliability is current obstacle of MEMS phase shifters; phase shifters using ferroelectric materials (BST) are another emerging technology.	CR	CR	CR
Advanced materials	New technologies for devices, structures, thermal, shielding.	CR	CR	CR
Advanced packaging	Die thinning and attachment technologies to enable the reliable, direct attachment of thinned die onto membrane; embedded electronics (vs. attachment alone) to embed the die in the structure for added reliability.	CR	E	E
Signal distribution	Technologies to simplify the interconnection of thousands of unit cells on the array; reliable RF, control, power, and data distribution; lightweight, low-loss, membrane-compatible interconnects for RF, data, and power distribution.	CR	E	E
Shielding for radiation tolerance	Since the conventional bulky package is not envisioned for the T/R module, the radiation protection of the device has to be accomplished through other methods of shielding.	CR	E	E
Passive and active thermal management	Radar-transparent thermal control coatings; variable emissivity surfaces/coatings; micro heat pipes.	CR	E	E
Power generation	Thin-film solar cells; power tiles for integrated and distributed power generation and storage on the membrane.	NR	E	E
Integrated passives	New technologies could replace the bulky energy storage capacitors with capacitor banks integrated directly in the membrane. This has the potential of lowering the complexity, mass, and cost of the antenna.	NR	CR	CR
Organic/printable electronics	Can be easily coated on flexible materials via simple processes such as ink-jet printing. A variety of molecular and polymeric materials may be used to construct thin-film transistors on a wide range of substrates.	NR	CR	CR
Large-scale manufacturing	Low-cost methods of attaching thousands of components on the membrane in such a way that the antenna is manufacturable, testable, and re-workable. Motivation for printing the electronics directly onto the membrane and integrating the remaining high-performance functions onto a single chip. New technologies such as roll-to-roll manufacturing processes are critical.	CR	CR	CR
System	Digital beamforming and digital TTD steering; calibration, metrology, and phase-correction.	CR	E	E

Table 6.4

Some of the key technologies that need to be further developed to enable advanced SAR missions of the next decade.

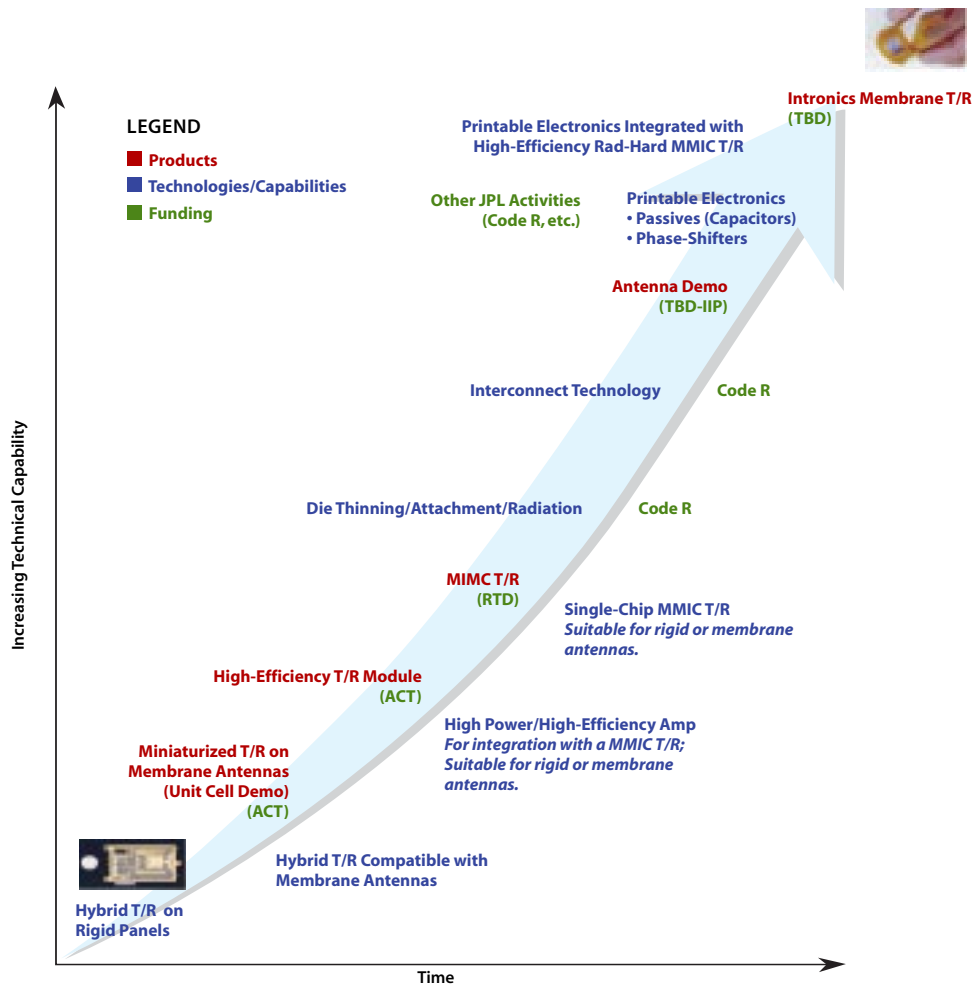
Legend

CR = Cost-reducing technology that will provide increased performance/capability

E = Enabling technology (required for mission feasibility)

NR = Not required for mission

Figure 6.8
Membrane
SAR technology
development plan.
Currently planned/
funded tasks and
relationship with
other programs
are shown in this
roadmap.



The roadmap shows the state of current technology, which is a conventionally packaged T/R module attached on a solid panel for SAR applications. The ultimate goal is to have a single flexible die integrated with the membrane. In this approach, only the parts of the T/R that cannot be printed onto the membrane are integrated onto the single chip.

One of the areas requiring additional investment is the interconnect technology. Lightweight, reliable, low-loss, membrane-compatible interconnects for RF, data, and

power distribution must be developed. Several candidate approaches exist and technology trades are required before selecting the optimal interconnect approach.

Continued research into membrane-compatible electronics is also required. The ultimate goal is a low-cost, reliable process for producing highly integrated, radiation-tolerant, mixed-signal circuits and attaching them reliably onto a membrane. This technology is critical for implementation of the GESS radar and would also enable many other large-aperture radar concepts.



National Aeronautics and
Space Administration

Jet Propulsion Laboratory
California Institute of Technology
Pasadena, California

JPL 400-1069 03/03